MERIT self-directed research report: Study of superconducting order parameter symmetry in iron-based superconductors with novel nematicity by terahertz spectroscopy

Kazuki Isoyama[1], Asato Onishi[2]

[1]Department of Physics, Graduate School of Science, The University of Tokyo
[2]Department of Advanced Materials Science, Graduate School of Frontier Sciences, The University of Tokyo

12, October, 2022

1 Introduction

Iron-based superconductor is one of the unconventional superconductors discovered in 2006. The paring mechanism of iron-based superconductors has been studied intensively since they show the second highest superconducting transition temperature (T_c) after cuprate superconductors under ambient pressure, and also show an anisotropic electronic response called (electronic) nematicity which is important for the study of other unconventional superconductors. $BaFe_2As_2$, a typical parent compound of iron-based superconductors, shows superconductivity in the electron-doped or hole-doped regime, and exhibits the nematic order with B_{2g} symmetry in the underdoped regime. On the other hand, in the hold-doped system $Ba_{1-x}A_xFe_2As_2$ ($A = K, Rb, Cs$), which may show the enhancement of electron correlation, nematic fluctuation with the B_{1g} symmetry has been reported for $x = 1$ end material [1,2]. Furthermore, in the overdoped regime of $0 < x < 1$, the symmetry of nematic susceptibility measured by the elastic resistivity measurement suggests the realization of a non-Ising-like nematic fluctuation (XY nematic), that is a novel nematic order different from both B_{2g} and B_{1g} nematicity [3]. In these hole-doped systems, isotropic A_{1g} susceptibility enhancement, which is different from the nematic symmetry, has also been reported [4]. Further study of the nature of the novel nematicity is required from the point of view of the connection with electronic correlations and superconductivity.

In this study, we investigate the correlation between the novel nematic order and the superconductivity in hole-doped systems, $Ba_{1-x}Rb_xFe_2As_2$, utilizing pump-probe spectroscopy. Pump-probe spectroscopy is a technique to excite the system by pump light and measure the excitation and relaxation dynamics by probe light, which allows us to observe the relaxation of the excited states to the ground state or metastable states by (sometimes selectively) exciting multiple orders with various energy scales, separated by different time constants. Studies on nematic ordering in iron-based superconductors by pump-probe scheme have been reported in electron-doped systems. In particular in the previous research [5], it has been reported that the reflectivity change of the probe light induced by the pump light (which is called the pump-probe signal), observed in the temperature region below the nematic

Rb concentration	a (Å)	c (Å)	T_c (K)	T_{nem} (K)
0.19	3.9436	13.218	15.6	101.5
0.67	3.8962	13.938	15	-
0.87	3.8762	14.239	6.2	40

Table 1. The compositions and properties of the samples.

transition temperature (T_{nem}), changes its sign below $T \sim T_c$, suggesting that the nematic order parameter is suppressed by the superconducting transition.

Initially, we aimed to study the correlation between the symmetry of the superconducting order parameter of $Ba_{1-x}Rb_xFe_2As_2$ and the nematic order by using terahertz (THz) electromagnetic wave, which has photon energy comparable to the superconducting gap energy ($\hbar\omega \sim$ meV) [6, 7]. However, we could not discuss the symmetry of the superconducting order parameter, because the observed signal measured in the THz pump-probe experiment was about one order of magnitude smaller than that estimated from previous studies. Therefore, we have changed our policy and aim at studying the relationship between the nematic and superconducting orders in $Ba_{1-x}Rb_xFe_2As_2$, such as whether they are competing or coexisting.

2 Experimental methods

First, $Ba_{1-x}Rb_xFe_2As_2$ single crystals are grown by the self-flux method, in which one of the precursors is melted at high temperature to serve as a solvent (flux) for the other precursors. We used FeAs as flux and BaAs and RbAs as precursors, and synthesized single crystals of various compositions by changing their mixing ratios based on the previous study [3].

The axis length and orientation of the synthesized samples were determined by the X-ray diffraction measurement, and T_c was evaluated by the electrical resistivity measurement. Since the axis length of $Ba_{1-x}Rb_xFe_2As_2$ varies linearly according to the Vegard law [8], the Rb concentration x of the sample was determined from the obtained a axis length[1].

The measured axis lengths of the samples and T_c and T_{nem} are summarized in Tab. 1. As shown in Fig. 1b, three samples used in this study are $x = 0.19$ with the B_{2g} nematic order, $x = 0.87$ with the B_{1g} nematic order, and $x = 0.67$ compound, in which XY-like nematic fluctuations are observed [3].

On the three compositions of the $Ba_{1-x}Rb_xFe_2As_2$ single crystals, visible light pump-near-infrared light probe spectroscopy was performed, and the time evolution of transient reflectance changes induced by visible light pulse was measured. Ultrashort pulse (pulse width 100 fs) at the wavelength of 800 nm (= 1.55 eV), output from a commercial Ti:sapphire regenerative amplifier (Coherent Libra), was used as the probe light pulse, and its second harmonic (wavelength of 400 nm = 3.10 eV) was used as the pump light pulse. The spot sizes of the pump and probe beam are 112 μm and 11 μm for the measurement of the $x = 0.19$ sample and 123 μm and 62 μm for the $x = 0.67$ and 0.87 samples, respectively. The excitation energy density was 260 μJ/cm^2 for the $x = 0.19$ sample and 100 μJ/cm^2 for the $x = 0.67$ and 0.87 samples.

Since $Ba_{1-x}Rb_xFe_2As_2$ has multiple excitation channels with different symmetry, the reflectivity change obtained in the pump-probe measurement is expected to depend on the polarization direction of the pump and probe pulse. Specifically, when the pump and probe light are incident perpendicular

[1] The a axis lengths of $BaFe_2As_2$ and $RbFe_2As_2$ are 3.9625 and 3.863 Å, respectively [9, 10].

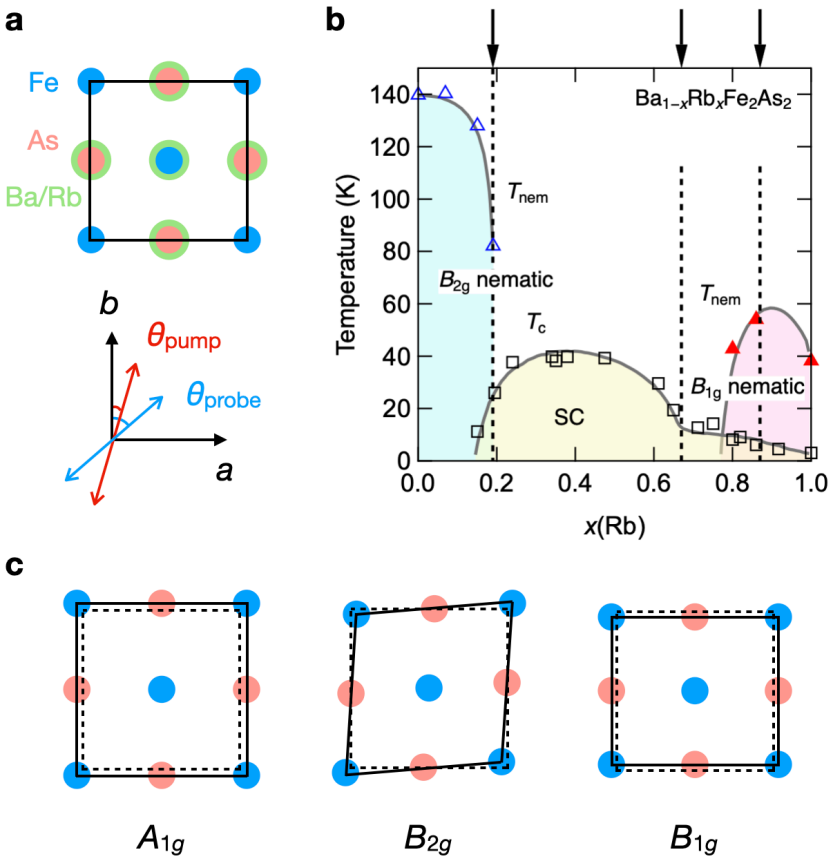

Figure 1. **a**: The crystal structure of $Ba_{1-x}Rb_xFe_2As_2$ (blue: Fe, red: As, green: Ba and Rb, which are located in the back side or front side of the paper) and the polarization configuration of the pump and probe light in the experiment. **b**: The phase diagram of $Ba_{1-x}Rb_xFe_2As_2$, reprinted from [3]. The compositions used in the measurement are shown by the black arrows. **c**: The three symmetry components appeared in the reflectivity change of $Ba_{1-x}Rb_xFe_2As_2$.

to the ab plane, the reflectivity change $\Delta R/R$ is decomposed into [11]

$$\frac{\Delta R}{R}(\theta_{\rm pump}, \theta_{\rm probe}) \propto \chi^{(3)}_{A_{1g}} + \chi^{(3)}_{B_{2g}} \sin 2\theta_{\rm pump} \sin 2\theta_{\rm probe} + \chi^{(3)}_{B_{1g}} \cos 2\theta_{\rm pump} \cos 2\theta_{\rm probe}, \qquad (1)$$

where $\chi^{(3)}_{A_{1g}}$, $\chi^{(3)}_{B_{2g}}$, and $\chi^{(3)}_{B_{1g}}$ are the the third-order nonlinear susceptibility with the A_{1g}, B_{2g}, and B_{1g} symmetry, respectively, and $\theta_{\rm pump}$ and $\theta_{\rm probe}$ are the polarization angles of the pump and probe pulse with respect to the crystal a axis (see Fig. 1a). In order to measure these multiple symmetry components separately, the reflectivity change was measured by changing the polarization direction of the pump and probe beams by using half wave plates.

3 Results and discussions

As a typical experimental result, Fig. 2 shows the dynamics of the reflectivity change in the $Ba_{1-x}Rb_xFe_2As_2$ ($x = 0.19$) sample and their decomposition into the dynamics of the nonlinear susceptibilities with the A_{1g}, B_{2g}, and B_{1g} symmetry, based on Eq. (1). As seen in Fig. 2, the dynamics of the nonlinear susceptibilities consists of a fast component that decays on the 1 ps timescale after the photoexcitation, followed by a slow component that remains over several contracts of 10 ps, which is similar for all samples and all temperatures. The fast component on the 1 ps timescale corresponds to the energy transfer from the electron system to the lattice system through the electron-lattice

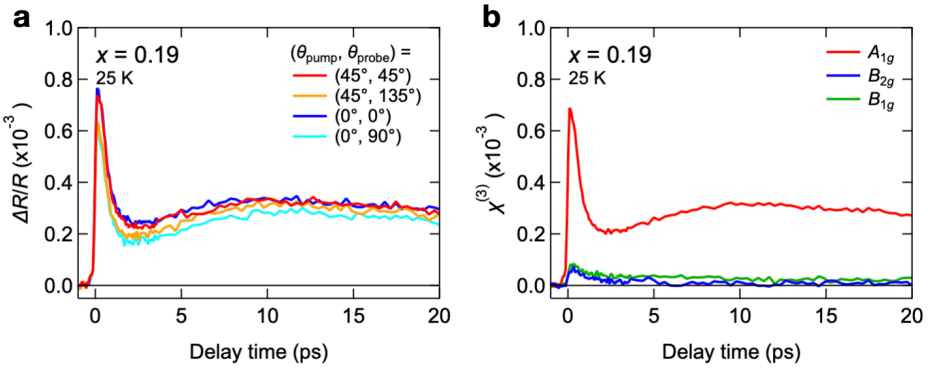

Figure 2. **a**: The reflectivity change dynamics of $Ba_{1-x}Rb_xFe_2As_2$ ($x = 0.19$), measured at 25 K. The polarization directions of the pump and probe pulse are changed. **b**: The decomposition of the reflectivity change dynamics (**a**) into the nonlinear susceptibility dynamics with the A_{1g}, B_{2g}, and B_{1g} symmetry, based on Eq. (1).

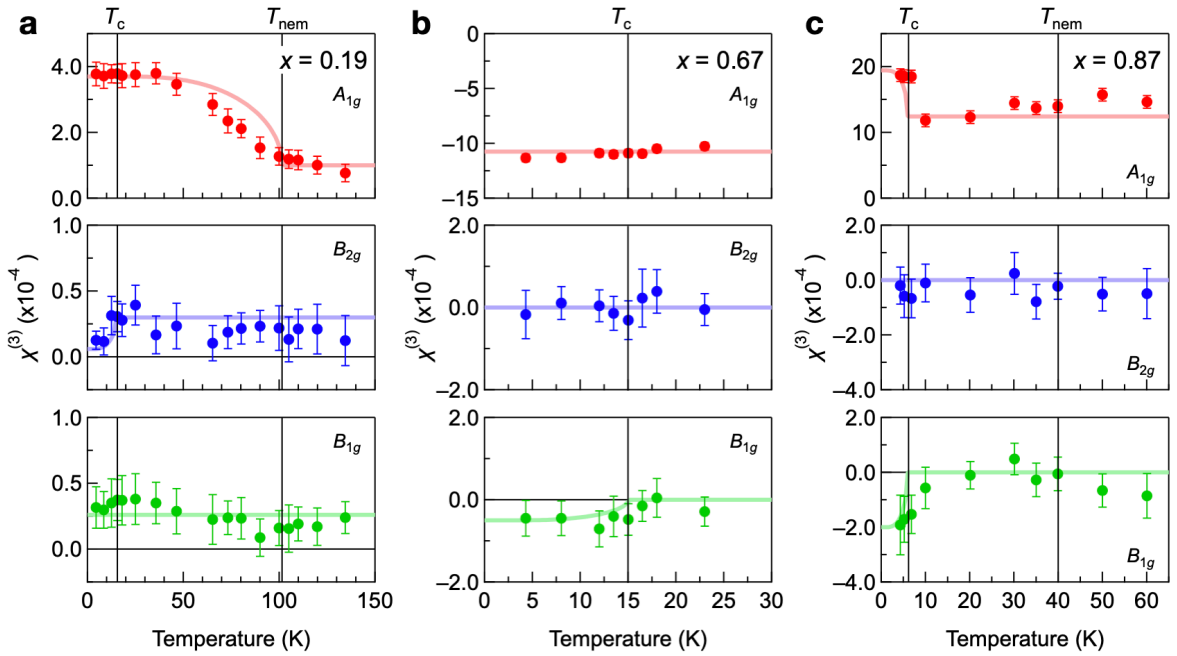

Figure 3. The temperature dependence of the magnitude of nonlinear susceptibility dynamics in **a**: $x = 0.19$, **b**: $x = 0.67$, and **c**: $x = 0.87$ samples, respectively. Fast components are shown in $x = 0.19, 0.87$ and slow component is shown in $x = 0.67$. Vertical lines indicate $T_c = 15.6$ K and $T_{nem} = 101.5$ K for $x = 0.19$, $T_c = 15.0$ K for $x = 0.67$, and $T_c = 6.2$ K and $T_{nem} = 40$ K for $x = 0.87$, respectively. Error bars represent the standard deviation and solid lines are guide to the eye.

interaction, and the slow component corresponds to the energy transfer from the lattice system to the heat bath, both of which are considered to reflect the photoexcitation dynamics of the nematic order. Since it is known that the dynamics of nematic order is prominent in the fast component with few ps decay [12], we obtained the temperature dependence of the magnitude of the nonlinear susceptibility dynamics as shown in Fig. 3 from the nonlinear susceptibility dynamics for each sample and temperature[2].

[2] The magnitude of the slow dynamics of the nonlinear susceptibility is obtained by averaging the dynamics for 10-15 ps. The magnitude of fast dynamics is obtained by averaging the dynamics for 0-1 ps and subtracting the slow component.

3.1 Result of $x = 0.19$ sample

First, as shown in Fig. 3a, a pump-probe signal was observed in the susceptibility of the A_{1g} symmetry $\chi^{(3)}_{A_{1g}}$ in the $x = 0.19$ sample with the B_{2g} nematic order at $T < T_{\rm nem}$, which reflects the photoexcitation dynamics of the nematic order. Furthermore, the B_{2g} signal $\chi^{(3)}_{B_{2g}}$ decrease at $T < T_{\rm c}$. Since the photoexcitation dynamics of the B_{2g} nematic order is expected to have a major contribution to the B_{2g} channel, this is considered to reflect a decrease of the nematic order parameter due to the superconducting transition, i.e., the competition between superconductivity and nematic order, similar to that observed in the previous work [5]. Note that the pump-probe signals obtained in this sample are nonzero for all symmetry components even at $T > T_{\rm nem}$. This is possibly because the intensity of the pump pump is about one order of magnitude stronger than the excitation intensity in the previous studies, and signals other than the excitation dynamics of the nematic order, such as interband transitions, are also captured.

3.2 Result of $x = 0.67$ sample

As mentioned in the introduction section, the composition of $x = 0.67$ does not exhibit long-range nematic orders, but exhibits XY nematic fluctuation, that is, non-Ising-like short-range nematic order [3], which makes us expect that the pump-probe signal of the $x = 0.67$ sample is independent to the temperature both in the B_{2g} and B_{1g} channels. However, contrary to such a simple expectation, a nonzero signal was observed in the B_{1g} channel at $T < T_{\rm c}$ (see the lower part of Fig. 3b). Also, in contrast to the B_{1g} signal, the B_{2g} signal was zero at the noise level at the measured temperature range. This result suggests that the B_{1g} nematic state is preferred to the B_{2g} state at $T < T_{\rm c}$. This result is not contradict to the previous dc elastic resistivity measurement, where Curie-Weiss like diverge of the nematic susceptibility toward lower temperature has been observed both in the B_{2g} and B_{1g} channels, which is considered to be XY nematic fluctuation [3], since the nematic susceptibility in the superconducting phase cannot be accessed by the dc resistivity measurement in principle. In other words, it is possible that the B_{1g} nematic phase grows under the superconducting phase, while the XY nematic state is realized in the short range at $T > T_{\rm c}$, where the nematic direction does not face a specific direction.

3.3 Result of $x = 0.87$ sample

The B_{1g} nematicity, whose the nematic direction is 45° tilted from that of the B_{2g} nematic phase, is realized in the $x = 0.87$ compound. In this composition, as shown in the lower panel of Fig. 3c, the emergence of the B_{1g} signal below $T < T_{\rm c}$ was observed, while the B_{1g} signal at $T > T_{\rm c}$ was almost zero, which does not match to the expectation that the signal originating from the B_{1g} nematic order will be observed in the B_{1g} channel in the temperature range of $T < T_{\rm nem}$. One reason why the B_{1g} signals was not observed in the temperature range of $T_{\rm c} < T < T_{\rm nem}$ may be explained by the size of the nematic domain. In the nematic phase, twin domains with the nematic direction along the a or b axis are coexisting. Since the spot size of the probe beam was 62 μm in diameter in this measurement, when the average domain size of the B_{1g} nematic phase is smaller than that, the pump-probe signals from the twins will cancel each other out. In fact, the typical domain size of the B_{2g} nematic phase in the $BaFe_2As_2$ system is about 10-100 μm [5, 13, 14], which is the same order of the spot size of the probe beam.

In contrast to the result at $T_c < T < T_{nem}$, the pump-probe signal in the B_{1g} channel was clearly observed in the temperature range of $T < T_c$. This result suggests that either the nematic order is enhanced by the emergence of the superconductivity at $T < T_c$, or that the signal cancellation due to the twin, mentioned previously, was solved by the superconducting transition. In the former case, a decrease of T_c has been observed in the region of $x > 0.8$ where the B_{1g} nematic order appears, suggesting a competition between the superconductivity and the B_{1g} nematicity [3]. However, recently, the enhancement of T_c by the nematic fluctuation has also been proposed in iron-based superconductors [15] and we cannot deny the possibility of the enhancement of the B_{1g} nematicity by the superconducting transition. The latter case, on the other hand, implies the growth of the domain size in the superconducting phase. Although the change of the domain size induced by the superconducting transition have not been observed in previous studies of the B_{2g} nematic phase, the B_{1g} nematic direction is considered to be coupled with the B_{1g} component of the macroscopic wave function that appears with the superconducting transition, and when this coupling is strong, the domain reformation and the accompanying growth of the domain size will be realized. Domain reformation associated with the superconducting transition is also suggested in the results for the composition of $x = 0.67$, and might be widely observed in the novel nematic phase in $Ba_{1-x}Rb_xFe_2As_2$.

4 Summary

In this study, we investigated the correlation between superconductivity and novel nematicity observed in the iron-based superconductor $Ba_{1-x}Rb_xFe_2As_2$ by utilizing the pump-probe spectroscopy. We synthesized three $Ba_{1-x}Rb_xFe_2As_2$ samples with different nematic orders by the self-flux method. By measuring the photo-induced reflectivity change, we observed a suppression of the nematic order parameter by the emergence of the superconducting order parameter in the composition of $x = 0.19$ with the B_{2g} nematic phase, which is commonly seen in iron-based superconductors. On the other hand, in the composition of $x = 0.87$ with the B_{1g} nematic phase, where the nematic direction is 45° different from that of the B_{2g} nematic phase, and in the composition of $x = 0.67$ with the XY nematic fluctuation, where the nematic direction does not point to a specific direction, we found that the pump-probe signal in the B_{1g} channel was observed only in the temperature range of $T < T_c$. This result suggests the emergence of the B_{1g} nematic order under $T < T_c$ in the overdoped regime of $Ba_{1-x}Rb_xFe_2As_2$ and the possible coexistence of the B_{1g} nematicity and superconductivity.

Both in the superconducting phase and in the normal phase, (angle resolved) photoemission spectroscopy are powerful tool to study the nematicity. For example in the previous study [14], nematicity waves with the wavelength of 0.5 μm, which is much smaller than the usual nematic domain size in iron-based superconductors, have been observed by utilizing a laser-based photoemission electron microscope. This method will enable us to detect the change of the nematic domain associated with the superconducting transition, suggested in this study. Also, in this study, pump-probe signals were observed even at $T > T_{nem}$, making difficult to extract the photoexcitaion dynamics of the nematicity from the pump-probe signal. In the composition of $x = 0.87$, no signal originating from nematic order was observed at $T_c < T < T_{nem}$, possibly because the spot size of the probe beam and domain size were comparable. In order to solve these problems, it would be effective to perform similar measurements under the conditions of low excitation density and small spot size by using a laser oscillator with a high repetition rate and high stability.

References

[1] Li, J. *et al.* Reemergeing electronic nematicity in heavily hole-doped Fe-based superconductors. *arXiv preprint arXiv:1611.04694* (2016).

[2] Liu, X. *et al.* Evidence of nematic order and nodal superconducting gap along [110] direction in $RbFe_2As_2$. *Nature communications* **10**, 1–12 (2019).

[3] Ishida, K. *et al.* Novel electronic nematicity in heavily hole-doped iron pnictide superconductors. *Proceedings of the National Academy of Sciences* **117**, 6424–6429 (2020).

[4] Wiecki, P. *et al.* Emerging symmetric strain response and weakening nematic fluctuations in strongly hole-doped iron-based superconductors. *Nature communications* **12**, 1–9 (2021).

[5] Thewalt, E. *et al.* Imaging Anomalous Nematic Order and Strain in Optimally Doped $BaFe_2(As, P)_2$. *Physical Review Letters* **121**, 027001 (2018).

[6] Katsumi, K. *et al.* Higgs Mode in the *d*-Wave Superconductor $Bi_2Sr_2CaCu_2O_{8+x}$ Driven by an Intense Terahertz Pulse. *Physical Review Letters* **120**, 117001 (2018).

[7] Grasset, R. *et al.* Terahertz pulse-driven collective mode in the nematic superconducting state of $Ba_{1-x}K_xFe_2As_2$. *npj Quantum Materials* **7**, 4 (2022).

[8] Peschke, S., Stürzer, T. & Johrendt, D. $Ba_{1-x}Rb_xFe_2As_2$ and Generic Phase Behavior of Hole-doped 122-Type Superconductors. *Zeitschrift für anorganische und allgemeine Chemie* **640**, 830–835 (2014).

[9] Rotter, M. *et al.* Spin-density-wave anomaly at 140 K in the ternary iron arsenide $BaFe_2As_2$. *Physical Review B* **78**, 020503 (2008).

[10] Bukowski, Z., Weyeneth, S., Puzniak, R., Karpinski, J. & Batlogg, B. Bulk superconductivity at 2.6 K in undoped $RbFe_2As_2$. *Physica C: Superconductivity and its applications* **470**, S328–S329 (2010).

[11] Boyd, R. W. *Nonlinear Optics* (Academic Press, 2008), third edn.

[12] Stojchevska, L., Mertelj, T., Chu, J.-H., Fisher, I. R. & Mihailovic, D. Doping dependence of femtosecond quasiparticle relaxation dynamics in $Ba(Fe,Co)_2As_2$ single crystals: Evidence for normal-state nematic fluctuations. *Physical Review B* **86**, 024519 (2012).

[13] Tanatar, M. A. *et al.* Direct imaging of the structural domains in the iron pnictides AFe_2As_2 (A = Ca, Sr, Ba). *Physical Review B* **79**, 180508 (2009).

[14] Shimojima, T. *et al.* Discovery of mesoscopic nematicity wave in iron-based superconductors. *Science* **373**, 1122–1125 (2021).

[15] Mukasa, K. *et al.* High-pressure Phase Diagrams of $FeSe_{1-x}Te_x$: Correlation between Suppressed Nematicity and Enhanced Superconductivity. *Nature Communications* **12**, 381 (2021).

Acknowledgements

We would like to express our sincere gratitude to our supervisors, Prof. Ryo Shimano and Prof. Takasada Shibauchi, for their great support and cooperation in conducting this research. We are grateful to our secondary supervisors in the MERIT program, Prof. Masao Ogata and Prof. Ryotaro Arita, for their kind permission to propose this research. We would like to take this opportunity to thank them. In addition, sample growth was conducted at National Institute of Advanced Industrial Science and Technology under the guidance of Dr. Shigeyuki Ishida, who gave us detailed consultation on the sample synthesis. In addition, during the period of the restriction of the admission due to the pandemic, we asked Dr. Ishida to synthesize the samples for us. We are very grateful to him.